Inorg. Chem. **2006**, *45*, 7091–7099

Indium Flux Synthesis of $RE_4Ni_2InGe_4$ (RE = Dy, Ho, Er, and Tm): An Ordered Quaternary Variation on the Binary Phase Mg_5Si_6

James R. Salvador and Mercouri G. Kanatzidis*

Department of Chemistry, Michigan State University, East Lansing, Michigan 48824

Received March 24, 2006

The quaternary compounds $RE_4Ni_2InGe_4$ (RE = Dy, Ho, Er, and Tm) were obtained as large single crystals in high yields from reactions run in liquid In. The title compounds crystallize in the monoclinic *C*2/*m* space group with the Mg_5Si_6 structure type with lattice parameters $a = 15.420(2)$ Å, $b = 4.2224(7)$ Å, $c = 7.0191(11)$ Å, and $\beta = 108.589(2)°$ for $Dy_4Ni_2InGe_4$, $a = 15.373(4)$ Å, $b = 4.2101(9)$ Å, $c = 6.9935(15)$ Å, and $\beta = 108.600(3)°$ for $Ho_4Ni_2InGe_4$, $a = 15.334(7)$ Å, $b = 4.1937(19)$ Å, $c = 6.975(3)$ Å, and $\beta = 108.472(7)°$ for $Er_4Ni_2InGe_4$, and $a = 15.253(2)$ Å, $b = 4.1747(6)$ Å, $c = 6.9460(9)$ Å, and $\beta = 108.535(2)°$ for $Tm_4Ni_2InGe_4$. $RE_4Ni_2InGe_4$ formed in liquid In from a melt that was rich in the rare-earth component. These compounds are polar intermetallic phases with a cationic rare-earth substructure embedded in a transition metal and main group matrix. The rare-earth atoms form a highly condensed network, leading to interatomic distances that are similar to those found in the elemental lanthanides themselves. The Dy and Ho analogues display two maxima in the susceptibility, suggesting antiferromagnetic ordering behavior and an accompanying spin reorientation. The Er analogue shows only one maximum in the susceptibility, and no magnetic ordering was observed for the Tm compound down to 2 K.

Introduction

Molten metals used as solvents to carry out reactions, most notably Al, have been found to produce complex intermetallics of the type RE/TM/Al and RE/TM/Al/Si or Ge (where RE is an rare-earth element and TM is a transition metal) with ubiquitous incorporation of Al atoms into the products.[1,2] Similarly, quaternary phases form readily in systems such as RE/TM/Ga/Ge[2,3] when excess Ga is used. It is, however, considerably more difficult to form the corresponding Ga/Si compounds, and reactions generally yield Ga-free products such as $SmNiSi_3$ and $RE_2Ni_{3+x}Si_{5-x}$,[4] though examples of quaternary phases have been reported.[5] By switching from Si to Ge and from Ga flux to In, we have observed parallels in reactivity where it appears to be increasingly more difficult to form quaternary phases in the RE/TM/In/Ge system just as in the corresponding Ga/Si systems. In fact, In can be used to recrystallize known ternary phases such as $YbNi_2Ge_2$ because it is not incorporated into the final products.[6] We have recently shown that reactions carried out in the RE/Ni/Ge system produce the phase β-$RENiGe_2$ in large quantities, with In acting as a nonreactive flux.[7] It is interesting that quaternary In-containing compounds such as $RE_4Ni_2InGe_4$ form rarely. In contrast, in Al flux reactions, the exclusion of Al from the final products has not been observed, resulting mainly in quaternary phases under similar

* To whom correspondence should be addressed. E-mail: kanatzid@cem.msu.edu.

(1) (a) Sieve, B.; Trikalitis, P. N.; Kanatzidis, M. G. *Z. Anorg. Allg. Chem.* **2002**, *628*, 1568−1573. (b) Sieve, B.; Sportouch, S.; Chen, X.-Z.; Cowen, J. A.; Brazis, P.; Kannewurf, C. R.; Papaefthymiou, V.; Kanatzidis, M. G. *Chem. Mater.* **2001**, *13*, 273−283. (c) Latturner, S. E.; Bilc, D.; Mahanti, S. D.; Kanatzidis, M. G. *Chem. Mater.* **2002**, *14*, 1695−1705. (d) Nieman, S.; Jeitschko, W. *J. Solid State Chem.* **1995**, *116*, 131−135. (e) Nieman, S.; Jeitschko, W. *J. Alloys Compd.* **1995**, *221*, 235−239. (f) Latturner, S. E.; Kanatzidis, M. G. *Inorg. Chem.* **2004**, *43*, 2−4. (g) Chen, X.-Z.; Sieve, B.; Henning, R.; Schultz, A. J.; Brazis, P.; Kannewurf, C. R.; Cowen, J. A.; Crosby, R.; Kanatzidis, M. G. *Angew. Chem., Int. Ed.* **1999**, *38*, 693−696. (h) Sieve, B.; Chen, X.-Z.; Cowen, J. A.; Larson, P.; Mahanti, S. D.; Kanatzidis, M. G. *Chem. Mater.* **1999**, *11*, 2451−2455.

(2) Kanatzidis, M. G.; Pöttgen, R.; Jeitschko, W. *Angew. Chem., Int. Ed.* **2005**, *44*, 6996−7023.

(3) (a) Chen, X.-Z.; Small, P.; Sportouch, S.; Zhuravleva, M.; Brazis, P.; Kannewurf, C. R.; Kanatzidis, M. G. *Chem. Mater.* **2000**, *12*, 2520−2522. (b) Zhuravleva, M. A.; Wang, X.; Schultz, A. J.; Bakas, T.; Kanatzidis, M. G. *Inorg. Chem.* **2002**, *41*, 6056−6061. (c) Zhuravleva, M. A.; Pcionek, R. J.; Wang, X. P.; Schultz, A. J.; Kanatzidis, M. G. *Inorg. Chem.* **2003**, *42*, 6412−6424.

(4) (a) Chen, X.-Z.; Larson, P.; Sportouch, S.; Brazis, P.; Mahanti, S. D.; Kannewurf, C. R.; Kanatzidis, M. G. *Chem. Mater.* **1999**, *11*, 75−83. (b) Zhuravleva, M. A.; Kanatzidis, M. G. *Z. Naturforsch. B* **2003**, *58*, 649−657.

(5) Zhuravleva, M. A.; Chen, X.-Z.; Wang, X. P.; Schultz, A. J.; Ireland, J.; Kannewurf, C. K.; Kanatzidis, M. G. *Chem. Mater.* **2002**, *14*, 3066−3081.

(6) Bud'ko, J. L.; Islam, Z.; Wiener, T. A.; Fisher, I. R.; Lacerda, A. H.; Canfield, P. C. *J. Magn. Magn. Mater.* **1999**, *205*, 53−78.

(7) Salvador, J. R.; Gour J. R.; Bilc, D.; Mahanti, S. D.; Kanatzidis, M. G. *Inorg. Chem.* **2004**, *43*, 1403−1410.

10.1021/ic0605017 CCC: $33.50
Published on Web 08/05/2006

conditions.[1,2] It is unclear at this stage why phases have failed to include In atoms in the structure despite the presence of a gross molar excess in the reactions. It may be that the shorter reaction times or moderate temperatures generally used in this chemistry help to stabilize kinetic phases. Alternatively, it may reflect a size effect of In or perhaps that soft polarizable metals such as In avoid the formation of bonds with harder elements such as Ge and Ni in accordance with the hard/soft acid/base theory of Pearson.[8] This is a fundamental reactivity issue worth exploring.

Here we report an example with successful incorporation of In into the structure of a phase containing Ge and a transition metal. The title compounds, $RE_4Ni_2InGe_4$, are the first reported, ordered quaternary intermetallic compounds containing a rare earth, a transition metal, In, and Ge. We detail the synthesis, stability, structure, and magnetic properties of the compounds $RE_4Ni_2InGe_4$ (RE = Dy, Ho, Er, and Tm) and discuss the dominant magnetic exchange mechanism in these systems.

Experimental Section

Reagents and Synthesis. An amount of 3 mmol of the corresponding RE metal (Er, Dy, and Tm were in the form of powder ground from a metal chunk; 99.9%, Chinese Rare-Earth Information Center, Inner Mongolia, China), Ho (250-mesh powder; 99.9%, Cerac, Milwaukee, WI), 1 mmol of Ni (−325 mesh; 99.9%, Cerac, Milwaukee, WI), 2 mmol of Ge (ground from 2−5-mm pieces; 99.999%, Plasmaterials, Livermore, CA), and 10 mmol of In (tear drops; 99.99%, Cerac, Milwaukee, WI) were combined in an alumina tube under an inert N_2 atmosphere in a glovebox. The reaction vessel and reactants were then flame-sealed in a fused-silica tube under a reduced atmosphere to prevent oxidation during heating. The samples were heated to 1000 °C over 10 h and held at that temperature for an additional 4 h. The temperature was then decreased to 850 °C and held for 48 h, and then the samples were cooled to room temperature over the course of 48 h. Product isolation from the excess In was accomplished by centrifugation of molten In through a coarse frit with subsequent immersion and sonication in glacial acetic acid for a period of 72 h. No deterioration of the product was observed by this method of isolation. The yields based on the starting quantities of Ni were 90−95%, with purity ranging from 60% to 80% depending on the RE metal. The phase identity and purity of polycrystalline samples were determined by powder X-ray diffraction.

The phase identity was assessed by comparing the experimental powder patterns to patterns calculated from the structural refinement using the CERIUS^2 suite of programs.[9] Impurity phases include binary REIn (with $REIn_3$) and a very small amount of Ni_5Ge_3. The reactions tended to favor higher yields of $RE_4Ni_2InGe_4$ for earlier rare-earth elements. The products grow as large silver bars, which tend to aggregate along the long axis.

We made several attempts to form $RE_4Ni_2InGe_4$ by direct combination by cold pressing of the elements in their stoichiometric ratios with heating in an induction furnace or arc-melting on a water-cooled Cu plate. These reactions were not successful in generating $RE_4Ni_2InGe_4$ for any of the rare-earth analogues.

Elemental Analysis. Semiquantitative microprobe elemental analysis was performed with a JEOL JSM-35C scanning electron microscope equipped with a Noran energy-dispersive spectrometer. Data were acquired with an accelerating voltage of 20 kV and 60-s acquisition times. Visibly clean surfaces were selected for analysis, and high magnifications were used during data collection in order to minimize the possibility of surface contamination by In not fully removed during the isolation process. A standardless quantitative elemental analysis on several crystals from the Dy reaction found an atomic composition of 40 (±1)% Dy, 10.2 (±0.8)% In, 35 (±1)% Ge, and 15 (±0.9)% Ni. This is in good agreement with the composition predicted by single-crystal X-ray diffraction analysis, which is 36% Dy, 9% In, 36% Ge, and 18% Ni. The likely reason for the small discrepancy in the Dy and Ni ratios may be due to the overlap of the Ni Kα line and the Dy L line in the X-ray fluorescence spectrum.

X-ray Crystallography. Single-crystal X-ray diffraction data were collected at room temperature using a Bruker AXS SMART CCD diffractometer with graphite-monochromatized Mo Kα (λ = 0.710 73 Å) radiation. Unit-cell refinement and data merging were done with the program *SAINT*, and an empirical absorption correction was applied using the program *SADABS*.[10] A monoclinic C-centered cell was found immediately from the data collected in the orientation matrix of the Ho analogue with lattice parameters that were quite similar to those of the orthorhombic I β-$ErNiGe_2$[7] but with a nonorthogonal angle (β = 108°). Inspection of the systematic absences for the full data set confirmed the initial finding that hkl, $h + k = 2n$, was the only extinction condition. This led to the possible space groups $C2$, Cm, and $C2/m$. The mean $|E^2 - 1|$ value of 0.819 was suggestive of a centrosymmetric space group, and so $C2/m$ was selected. The structure of $Ho_4Ni_2InGe_4$ was solved by direct methods, and the final structural refinement was performed with *SHELXTL*.[11] The In site was found to have rather large anisotropic temperature factors, and the occupancy of the site was refined and found to be nearly fully (>96%) occupied. Subsequent solutions of other RE analogues were obtained by using the atomic coordinates from $Ho_4Ni_2InGe_4$ and subsequent refinement with *SHELXTL*. Similar refinements of the In site were done on the other analogues, and all were found to be 96% occupied or higher. The data collection and refinement details for $RE_4Ni_2InGe_4$ are given in Table 1. The atomic positions and isotropic displacement parameters are listed in Table 2.

Magnetic Measurements. Magnetic susceptibility measurements were made on manually selected crystals from samples that had been screened by powder X-ray diffraction. Measurements were performed with a Quantum Design MPMS SQUID magnetometer in both field-cooled and zero-field-cooled settings at temperatures between 2 and 300 K with an applied field of 2000 Oe for $Dy_4Ni_2InGe_4$, 500 Oe for the Ho analogue, and 1000 Oe for $Er_4Ni_2InGe_4$ and $Tm_4Ni_2InGe_4$. Additionally, magnetization measurements were made at 2 K with field sweeps from −55 to +55 kOe at 2 K for all analogues. Diamagnetic corrections were made to the data for core electron contribution and for susceptibility of the container.[12]

Results and Discussion

Reaction Chemistry. $Ho_4Ni_2InGe_4$ (the first member to be synthesized) was originally found in a reaction designed

(8) Pearson, R. G. *Chemical Hardness: Applications from Molecules to Solids*; Wiley-VCH: New York, 1997.

(9) *CERIUS^2*, Version 1.6; Molecular Simulations Inc.: Cambridge, England, 1994.

(10) *SAINT*, Version 4; Bruker Analytical X-ray Instruments, Inc.: Madison, WI. Sheldrick, G. M. *SADABS*; University of Göttingen: Göttingen, Germany.

(11) *SHELXTL*, Version 6.10; Bruker Analytical X-ray Instruments, Inc.: Madison, WI, 2001.

(12) Selwood, P. W. *Magnetochemistry*, 2nd ed.; Interscience Publishers: New York, 1956; p 70.

Table 1. Crystallographic Data for $RE_4Ni_2InGe_4$ (RE = Dy, Ho, Er, and Tm), Space Group C2/*m*

empirical formula	$Dy_4Ni_2InGe_4$	$Ho_4Ni_2InGe_4$	$Er_4Ni_2InGe_4$	$Tm_4Ni_2InGe_4$
fw	1172.6	1182.32	1191.4	1198.32
a (Å)	15.420(2)	15.373(4)	15.334(7)	15.253(2)
b (Å)	4.2224(7)	4.2101(9)	4.194(2)	4.1747(6)
c (Å)	7.0191(11)	6.9935(15)	6.975(3)	6.9460(9)
β (deg)	108.589(2)	108.600(3)	108.472(7)	108.535(2)
V (Å^3)/*Z*	433.18(12)/2	428.99/2	425.4(3)/2	419.3(1)/2
d_{calcd} (g cm^{-3})	8.99	9.15	9.30	9.49
abs coeff (mm^{-1})	54.4	57.0	59.7	62.9
index ranges	$-19 \le h \le +20$, $-5 \le k \le +5$, $-9 \le l \le +8$	$-19 \le h \le +19$, $-5 \le k \le +5$, $-9 \le l \le +9$	$-19 \le h \le +19$, $-5 \le k \le +5$, $-9 \le l \le +9$	$-19 \le h \le +19$, $-5 \le k \le +5$, $-8 \le l \le +8$
reflns collected/unique/*R*(int)	2310/551/0.0323	1779/549/0.0256	2379/555/0.0287	2212/536/0.0285
data/restraints/param	551/0/36	549/0/36	555/0/36	536/0/36
GOF on F^2	1.177	1.230	1.228	1.214
final *R* indices [$I > 2\sigma(I)$] (R1/wR2)[a]	0.0222/0.0540	0.0281/0.0685	0.0218/0.0508	0.0237/0.0582
R indices (all data) (R1/wR2)[a]	0.0233/0.0544	0.0302/0.0694	0.0237/0.0512	0.249/0.0587

[a] $R1 = \sum||F_o| - |F_c||/\sum|F_o|$ and $wR2 = [\sum(|F_o^2 - F_c^2|)^2/\sum(wF_o^2)^2]^{1/2}$.

Table 2. Atomic Coordinates ($\times 10^4$) and Equivalent Isotropic Displacement Parameters (Å$^2 \times 10^3$) for $RE_4Ni_2InGe_4$ (RE = Dy, Ho, Er, and Tm)

atom	Wyckoff	*x*	*y*	*z*	*U*(eq)[a]
Dy(1)	4i	4088(1)	0	6107(1)	4(1)
Dy(2)	4i	3448(1)	0	0624(1)	4(1)
In	2d	5000	5000	0	8(1)
Ge(1)	4i	2033(1)	0	2701(2)	5(1)
Ge(2)	4i	5644(1)	5000	6617(2)	4(1)
Ni	4i	2168(1)	0	6432(2)	7(1)
Ho(1)	4i	4086(1)	0	6100(1)	6(1)
Ho(2)	4i	3446(1)	0	0629(1)	7(1)
In	2d	5000	5000	0	10(1)
Ge(1)	4i	2026(1)	0	2683(2)	7(1)
Ge(2)	4i	5645(1)	5000	6620(2)	7(1)
Ni	4i	2170(1)	0	6427(3)	10(1)
Er(1)	4i	4091(1)	0	6107(1)	5(1)
Er(2)	4i	3447(1)	0	0633(1)	5(1)
In	2d	5000	5000	0	9(1)
Ge(1)	4i	2018(1)	0	2659(2)	6(1)
Ge(2)	4i	5649(1)	5000	6618(2)	6(1)
Ni	4i	2176(1)	0	6407(2)	8(1)
Tm(1)	4i	4094(1)	0	6112(1)	5(1)
Tm(2)	4i	3447(1)	0	0633(1)	6(1)
In	2d	5000	5000	0	10(1)
Ge(1)	4i	2009(1)	0	2629(2)	6(1)
Ge(2)	4i	5652(1)	5000	6623(2)	6(1)
Ni	4i	2181(1)	0	6384(2)	8(1)

[a] *U*(eq) is defined as one-third of the trace of the orthogonalized $\mathbf{U}^{ij}$ tensor.

Table 3. Bond Lengths [Å] for $RE_4Ni_2InGe_4$ (RE = Dy, Ho, Er, and Tm)

	RE = Dy	RE = Ho	RE = Er	RE = Tm
RE(1)−Ge(2)	2.9645(9)	2.9537(12)	2.9412(12)	2.9296(10)
RE(1)−Ge(1)	3.0108(9)	3.0008(12)	2.9923(12)	2.9811(10)
RE(1)−Ni	3.0306(11)	3.027(2)	3.0086(19)	2.9836(16)
RE(1)−Ni	3.0404(16)	3.0182(14)	3.0143(13)	2.9998(12)
RE(1)−Ge(2)	3.1298(10)	3.1218(12)	3.1135(13)	3.0972(10)
RE(1)−Ge(1)	3.3054(13)	3.3042(17)	3.3232(17)	3.3279(14)
RE(1)−In	3.3840(5)	3.3761(7)	3.3636(11)	3.3450(5)
RE(2)−Ge(2)	2.9052(9)	2.8931(12)	2.8826(12)	2.8658(9)
RE(2)−Ni	2.9747(15)	2.967(2)	2.9744(18)	2.9697(16)
RE(2)−Ge(1)	2.9860(13)	2.9728(17)	2.9607(16)	2.9441(14)
RE(2)−Ge(1)	3.0580(10)	3.0416(13)	3.0230(13)	2.9959(10)
RE(2)−Ni	3.2988(12)	3.2882(16)	3.2903(14)	3.2907(13)
RE(2)−In	3.3233(5)	3.3164(7)	3.3054(11)	3.2900(5)
RE(2)−RE(2)	3.4843(9)	3.4698(11)	3.4629(13)	3.4440(9)
In−Ge(2)	2.8511(12)	2.8395(16)	2.8356(15)	2.8238(13)
In−Ge(1)	3.1038(12)	3.0806(16)	3.0622(16)	3.0275(13)
Ge(1)−Ni	2.4221(9)	2.4199(12)	2.4164(12)	2.4116(10)
Ge(1)−Ni	2.560(2)	2.556(3)	2.547(2)	2.536(2)
Ge(2)−Ni	2.3951(19)	2.392(2)	2.393(2)	2.3902(19)
Ge(2)−Ge(2)	2.494(2)	2.490(3)	2.492(2)	2.487(2)

to produce β-$HoNiGe_2$. The starting materials used for this synthesis were Ho in the form of large foil chunks, finely ground Ni and Ge powder, and In "teardrops" and were mixed in a ratio of 1:1:2:10, respectively. A small quantity (yields < 10%) of clustered needles were obtained from these original reactions. The product exhibited a crystal habit similar to that of β-$HoNiGe_2$; however, elemental analysis and X-ray diffraction showed these crystals to be of a different structure and composition.

After the stoichiometry was assessed by elemental analysis and X-ray diffraction, reactions were carried out by combining finely ground Ho, Ni, and Ge in their stoichiometric ratios in a 5-fold excess of In. These reactions yielded only β-$HoNiGe_2$; however, when the amount of Ho powder was increased by 50% in subsequent reactions, $Ho_4Ni_2InGe_4$ was obtained in 70% yield without the production of α- or β-$HoNiGe_2$, $HoNi_2Ge_2$, or RE_2InGe_2.[13] Other RE analogues could also be synthesized in high yield by adding an excess of finely ground RE metal to the reaction.

We rationalize this finding by considering that $Ho_4Ni_2InGe_4$ was first identified in reactions where large pieces of Ho were used as a reagent, and therefore it is likely that the kinetics of Ho metal dissolution was slow. The slowly dissolving Ho chunk could give rise to large local concentrations of Ho metal in the molten In, and it may in fact be this kinetically elevated Ho concentration that stabilized $Ho_4Ni_2InGe_4$. Therefore, to obtain $Ho_4Ni_2InGe_4$ in high yield, excess Ho powder is required to create the higher Ho concentrations such as those present in the original reaction. However, the RE-to-Ni ratio in the title compounds is 2:1, and so perhaps a high RE-to-Ni ratio favors the formation of the compounds. These results demonstrate that it is possible in some cases for liquid In to act as a reactive flux in reactions containing group 14 elements.

Structure. Because of the isostructural nature of the compounds, the structure will be described in terms of the $Ho_4Ni_2InGe_4$ analogue with regard to bond distances. Selected bond distances for all compounds are listed in Table 3. $RE_4Ni_2InGe_4$ crystallizes in the monoclinic space group *C*2/*m* with the Mg_5Si_6 structure type. In fact, $RE_4Ni_2InGe_4$

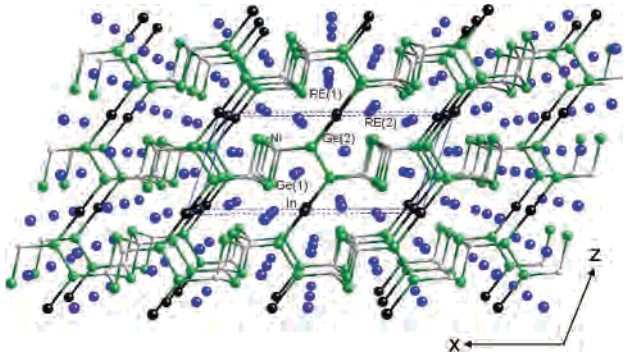

Figure 1. Structure of $RE_4Ni_2InGe_4$ as viewed along the *b*-axis. The blue circles represent the RE atoms, the gray circles are Ni atoms, the black circles are In atoms, and the green circles are Ge atoms.

is the first example of a compound produced in bulk to adopt the Mg_5Si_6 structure type.[14] Mg_5Si_6 has not been synthesized in pure form, to the best of our knowledge, but it has been identified as an intermetallic phase forming micron-sized islands in an Al matrix of Al-based alloys, and its structure was elucidated by area-selected electron diffraction methods.[14] $RE_4Ni_2InGe_4$ is an ordered variant of this binary phase, with the RE and In atoms occupying the Mg positions and Ni and Ge adopting the Si sites. The fact that the quaternary phase orders in this way is consistent with the more electropositive nature of RE and In (compared to Ni and Ge) and that they are more likely to adopt the Mg sites within the compound. From previous reports, it is well established that Ni will substitute for Si in intermetallic compounds[1] and as Ge is in the same group as Si, it is not surprising that Ni and Ge order on the Si sites.

The overall structure is shown in Figure 1. The substructure of $[Ni_2InGe_4]$ is a three-dimensional framework with channels, in which rare-earth ions are situated. These channels can be thought of as being composed of Ge(2) dimers, $Ni_2Ge(1)_2$ ribbons, and In atoms, as shown in Figure 2A. The Ge(2) atoms that form the dimers find themselves in a trigonal-planar environment of Ge and Ni atoms, a common geometry in intermetallic compounds when one neglects the rare-earth contacts.[15] The Ge−Ge distance of this dimer is 2.490(3) Å and compares well to other Ge−Ge bonds in trigonal-planar environments, for example, those found in β-$RENiGe_2$,[7] which average 2.495 Å, and in compounds that adopt the Ce_2CuGe_6 structure type,[16] whose Ge−Ge distances are in the range of 2.477 Å. Despite the Ge_2 dimer exhibiting a trigonal-planar environment reminiscent of sp^2-hybridized double-bonding arrangements, the bond distances in $RE_4Ni_2InGe_4$ (Table 3) are too long to be considered a Ge−Ge double bond because literature values for Ge−Ge double bonds are closer to 2.3 Å.[17] In fact, the Ge_2 dimer distances in the title compounds compare well with other Ge dimers where the Ge atoms are tetrahedral, which are typically 2.49−2.51 Å.[15]

The $Ni_2Ge(1)_2$ double chains (or ribbons) run along the monoclinic *b* axis. The ribbons are made of fused Ni_2Ge_2 rhombi, as highlighted in Figure 2C. The Ni−Ge(1) atoms form three bonds with distances of 2.4199(12) Å (×2) and 2.556(3) Å. The final structural moiety is a linear Ge(2)−In−Ge(2) segment formed by the In atom serving as a bridge to the Ge dimers (Figure 2A). The In−Ge(2) distance is 2.840(2) Å. This distance compares well to corresponding distances found in RE_2InGe_2.[13] In this compound, the In atoms are in a square-planar environment with a distance of 2.876 Å. The Zintl phases SrInGe[18] and $Ca_2LiInGe_2$[19] have In−Ge bonds that range from 2.751(2) to 2.887(1) Å, though In is tetrahedrally coordinated in these examples. The resulting linear Ge−In−Ge moiety in the title compound is unique. It serves to connect the $Ni_2Ge(1)_2$-based ribbons by forming bonds between Ni and Ge(2) with a distance of 2.392(2) Å (Figure 2B). The Ni atom within the "Ni_2InGe_4" framework has a distorted tetrahedral environment, a common coordination geometry found in a wide range of structure types such as $RENi_2Ge_2$[15] and $BaNiSn_3$.[20]

The linearly coordinated In atom, which resides on the 2d Wyckoff position, is highly unusual. If the very long interaction between Ge(1) and In were also considered bonding [3.081(2) Å], the In atom is then in a distorted square-planar environment similar to that found in RE_2InGe_2,[13] which is also uncommon because In is often tetrahedrally coordinated when bound to four other atoms.[18,19] We have taken great care to determine that this position is in fact an In atom and not a partially occupied Ho site (or other RE in subsequent crystal structures). The bond distances, the fact that the site refines better as a fully occupied In site rather than as a partially occupied (68%) Ho site, and the presence of In in the compound as shown by elemental analysis are consistent with our formula.[21]

The coordination environments of the two crystallographically distinct RE atoms are quite different from one another. The coordination environments out to 3.4 Å for RE(1) and RE(2) are illustrated in parts A and B of Figure 3, respectively. RE(1) is 11-coordinate, making three bonds to Ni, six bonds to Ge [four to Ge(2) and two to Ge(1)] and two bonds to In atoms, respectively. RE(2), on the other hand, is only 8-coordinate, forming five bonds to Ge [three

(13) (a) Zaremba, V. I.; Tyvanchuk, Yu. B.; Stepien-Damm, Yu. *Z. Kristallogr.* **1997**, *212*, 291−291. (b) Tobash, T. J.; Lins, D.; Bobev, S.; Lima, A.; Hundley, M. F.; Thompson, J. D.; Sarrao, J. L. *Chem. Mater.* **2005**, *17*, 5567−5573. (c) Zaremba, V. I.; Kaczorowski, C.; Nychyporuk, G. P.; Rodewald, U. C.; Pöttgen, R. *Solid State Sci.* **2004**, *6*, 1301−1306. (d) Zaremba, V. I.; Johrendt, D.; Rodewald, U. Ch.; Nychyporuk, G. P.; Pöttgen, R. *Solid State Sci.* **2005**, *7*, 998−1002.
(14) (a) Zandergen, H. W.; Andersen, S. J.; Jansen, J. *Science* **1997**, *277*, 1221−1225. (b) Andersen, S. J.; Zandergen, H. W.; Jansen, J.; Traeholt, C.; Tundal, U.; Reiso, O. *Acta Mater.* **1998**, *46*, 3283−3298.
(15) Szytula, A.; Leciejewicz, J. *Handbook of Crystal Structure and Magnetic Properties of Rare Earth Intermetallics*; CRC Press: Boca Raton, FL, 1994.
(16) Kony, N. B.; Salamakha, P. S.; Bodak, O. I.; Pecharskii, V. K. *Kristallografiya* **1988**, *33*, 838−840.
(17) Richards, A. F.; Marcin Brynda, M.; Power, P. P. *Chem. Commun.* **2004**, *14*, 1592−1593.
(18) Mao, J.-G.; Goodey, J.; Guloy, A. M. *Inorg. Chem.* **2002**, *41*, 931−937.
(19) Mao, J.-G.; Xu, Z.; Guloy, A. M. *Inorg. Chem.* **2001**, *40*, 4472−4477.
(20) Doerrscheidt, W.; Schaefer, H. *J. Less-Common Met.* **1978**, *58*, 209−216.
(21) The *R* values for the partially occupied Ho model are 0.0286 and 0.0703 for R1 and wR2, respectively, compared to 0.0281 and 0.0679 for the fully occupied In model. Additionally, the thermal parameters are 50% higher than those of the coordinating Ge atoms when the system is modeled as a partially occupied Ho atom.

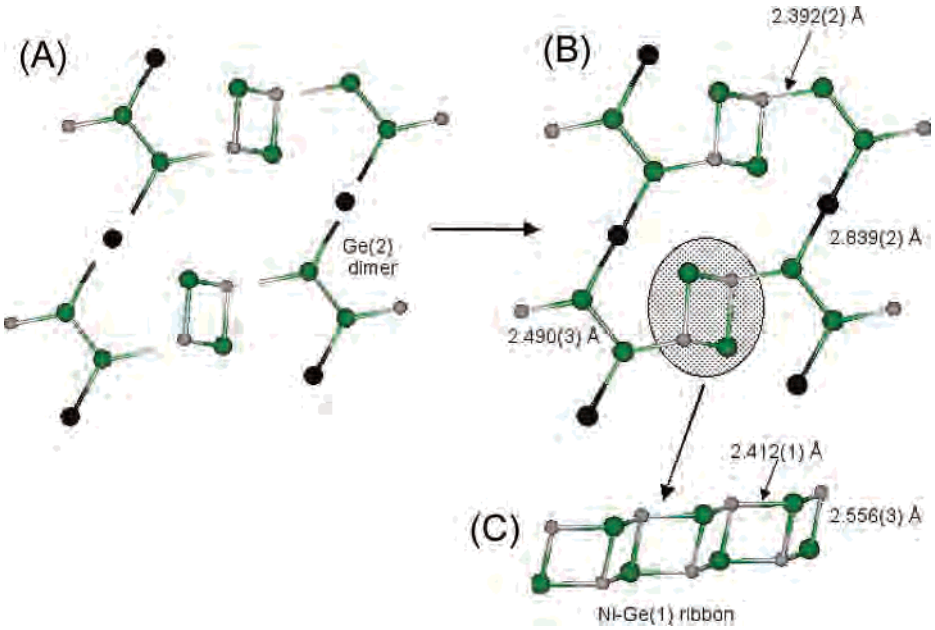

Figure 2. (A) Ni_2InGe_4 substructure decomposed into recognizable subunits of the Ge(2) dimer, the $Ni_2Ge(1)_2$ ribbon, and the linearly coordinated In atom. (B) Same building units condensed to form the channel network in which the RE ions reside. The shaded oval area indicates the $Ni_2Ge(1)_2$ ribbon viewed along its length. (C) $Ni_2Ge(1)_2$ ribbon.

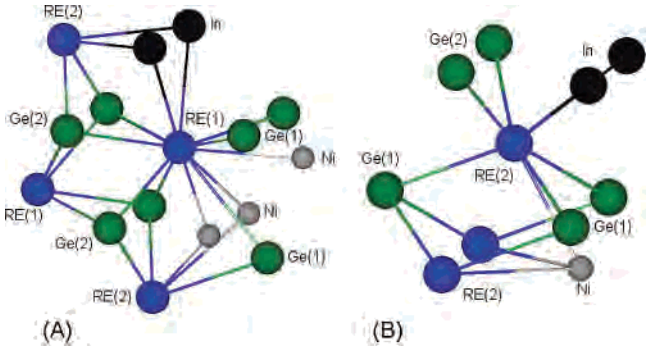

Figure 3. (A) Coordination environment of RE(1) atoms including the second neighbors. (B) Coordination environment of RE(2) atoms with second neighbors. The coordination sphere cutoff is 3.4 Å.

to Ge(1) and two to Ge(2)], two to In, and one to Ni. In the Ho analogue, the distances between the rare-earth atoms range from 3.4698(12) Å for Ho(2)−Ho(2) to ∼3.61 Å for Ho(1)−Ho(1) and Ho(1)−Ho(2). These distances are close to the 3.4-Å contacts found in elemental Ho.[22] The RE−RE distances for the other analogues are given in Table 3.

Magnetic Properties. The rare-earth ions in $RE_4Ni_2InGe_4$ are in much closer proximity than in many other rare-earth-containing intermetallics.[15] In the present case, the inter-rare-earth distances range from 3.4 to 3.6 Å and are comparable to those found in the RE metals themselves.[22] Analysis of the susceptibility data reveals a strong coupling between the moments, especially in the Dy analogue; this results in interesting magnetic ordering and spin reorientation within the magnetic domains of $RE_4Ni_2InGe_4$. Below we present the temperature-dependent magnetic susceptibility data for all compounds and show that definitive trends exist. We follow with a discussion of the origin of these trends on the basis of conduction-electron-mediated magnetic coupling and the so-called de Gennes factor.

(a) $Dy_4Ni_2InGe_4$. The magnetic susceptibility data for $Dy_4Ni_2InGe_4$ are shown in Figure 4A. The inverse susceptibility data obey the Curie−Weiss law from 35 to 300 K, with a resulting effective magnetic moment of 21.7 μ_B per formula unit. This is in good agreement with the value calculated for four independent Dy^{3+} ions, which is 21.4 μ_B.[23] The Weiss constant was determined to be −35.9 K, indicating antiferromagnetic interactions between the Dy^{3+} ions. At approximately 30 K, the susceptibility reaches a maximum, below which it decreases before increasing again below 27 K and then rising to a second maximum at 11 K. This results in a saddle curve between 30 and 11 K (Figure 4A). Below this temperature, the susceptibility decreases down to 2 K. Several samples were measured, and it was found that this double-maximum behavior in the susceptibility data was fully reproducible. Indeed, measurements were made on a single-crystal sample previously screened by X-ray diffraction to verify that it consisted of a single-crystallographic domain, and qualitatively identical results were obtained. While it is well established that single-crystallographic domains may contain many magnetic domains, the fact that the sample was a single crystal implies sample purity and that this double-maximum behavior is not due to the alignment of different crystallographic axes with the magnetic field. The two maxima observed in the data strongly suggest that the compound orders antiferromagnetically and then undergoes a spin reorientation at lower temperature, resulting in a second maximum in the susceptibility data.

Figure 4B shows the magnetization curve for $Dy_4Ni_2InGe_4$. At low fields, the moment is weakly dependent on the applied field. At 16.3 kOe, the slope of the magnetization increases,

(22) Donohue, J. *The Structures of the Elements*; Wiley: New York, 1974.
(23) Kittel, C. *Introduction to Solid State Physics*, 7th ed.; Wiley: New York, 1996.

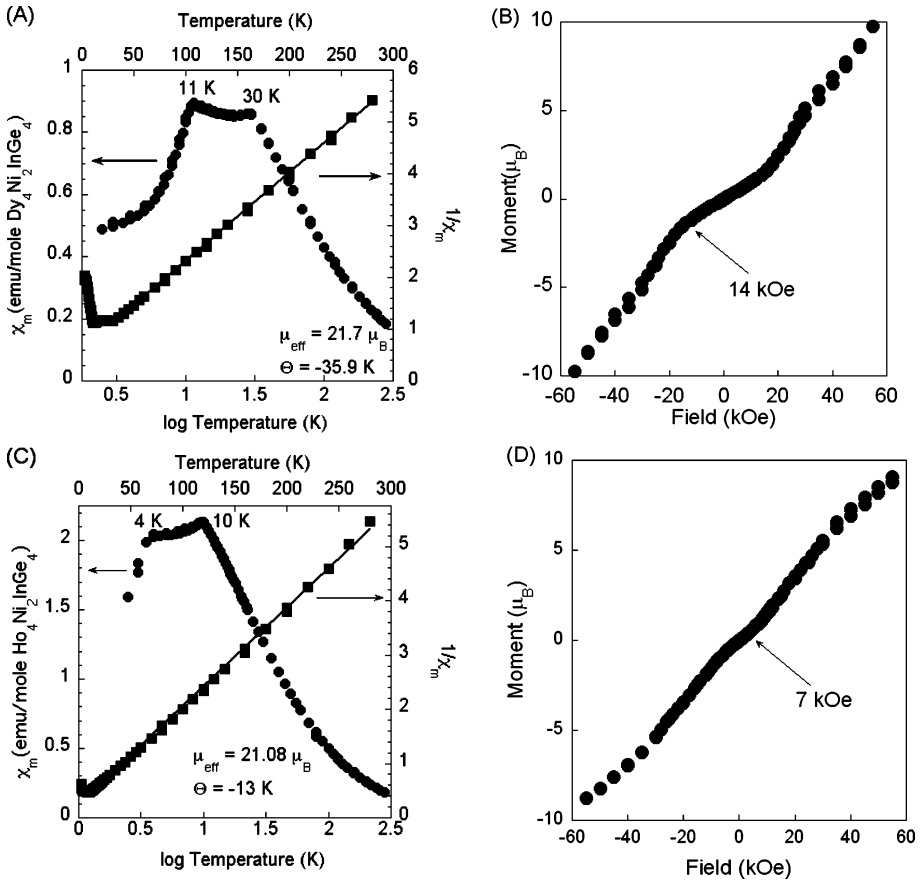

Figure 4. (A) Magnetic susceptibility vs log of the temperature and inverse susceptibility data vs temperature for $Dy_4Ni_2InGe_4$. The log of the temperature data highlights the "saddle" generated by the two maxima in the low-temperature region. (B) Field-dependent magnetization data for $Dy_4Ni_2InGe_4$ collected at 2 K. (C) magnetic susceptibility vs log of the temperature and inverse susceptibility data vs temperature for $Ho_4Ni_2InGe_4$. The log of the temperature data emphasizes the low-temperature behavior of this compound. (D) Field-dependent magnetization data for $Ho_4Ni_2InGe_4$ collected at 2 K.

which could be due to a metamagnetic transition, where the field disrupts the antiferromagnetic order. After the order is disrupted, the system behaves as a typical paramagnet, with a linear increase of the moment with applied field. The compound gives no indication of saturation at the highest attainable field because it continues to increase linearly up to 55 kOe, reaching only about 55% of the calculated saturation value.

(b) $Ho_4Ni_2InGe_4$. The magnetic and inverse susceptibility data for $Ho_4Ni_2InGe_4$ are shown in Figure 4C. The Ho analogue also displays the double-maximum behavior at low temperatures. Again this is suggestive of antiferromagnetic ordering with an accompanying spin reorientation. A first maximum is reached in the susceptibility data at 10 K, below which the susceptibility decreases slowly until 4 K, at which point, after a small upturn, the susceptibility decreases much more quickly down to 2 K. Above 10 K, the susceptibility data follow the Curie−Weiss law, with a resulting effective magnetic moment of 21.08 μ_B per formula unit and a Weiss constant of −13 K. The effective magnetic moment obtained from the inverse susceptibility data is in excellent agreement with the theoretical value of 21.2 μ_B predicted for four Ho^{3+}-cations.[23] The negative Weiss constant (θ) again indicates antiferromagnetic interactions. The double-maximum behavior observed for $Ho_4Ni_2InGe_4$ was reproducible with several samples.

The magnetization curve for $Ho_4Ni_2InGe_4$ is shown in Figure 4D. It is qualitatively similar to the magnetization curve measured for the Dy analogue. In the low-field regions, there is a weaker dependence of the moment on the applied field until again a critical field is reached at 7.0 kOe; then there is an increase in the slope. The magnetization increases linearly above the critical field up to the highest fields attainable, giving no indication of saturation and again reaching only 50% of the full value.

(c) $Er_4Ni_2InGe_4$. The magnetic and inverse susceptibility for $Er_4Ni_2InGe_4$ are shown in Figure 5A. The behavior of this compound is different from that of the previous two cases in that we observe only one maximum in the susceptibility data, which appears at 5 K and suggests an antiferromagnetic ordering with no spin reorientation. The data follow a Currie−Weiss law at temperatures greater than 100 K. Below this temperature, the data negatively diverge. The effective magnetic moment obtained from the inverse susceptibility data above 100 K resulted in a moment of 18 μ_B per formula unit with a Weiss constant of −7 K. The moment obtained from the data is in reasonably good agreement with the calculated value for four Er^{3+} centers of 19 μ_B.[23]

The magnetization curve for $Er_4Ni_2InGe_4$ is shown in Figure 5B. Once again, in the low-field region of the magnetization data, the moment has a weak dependence on the applied field. At a critical field of about 4.6 kOe, there

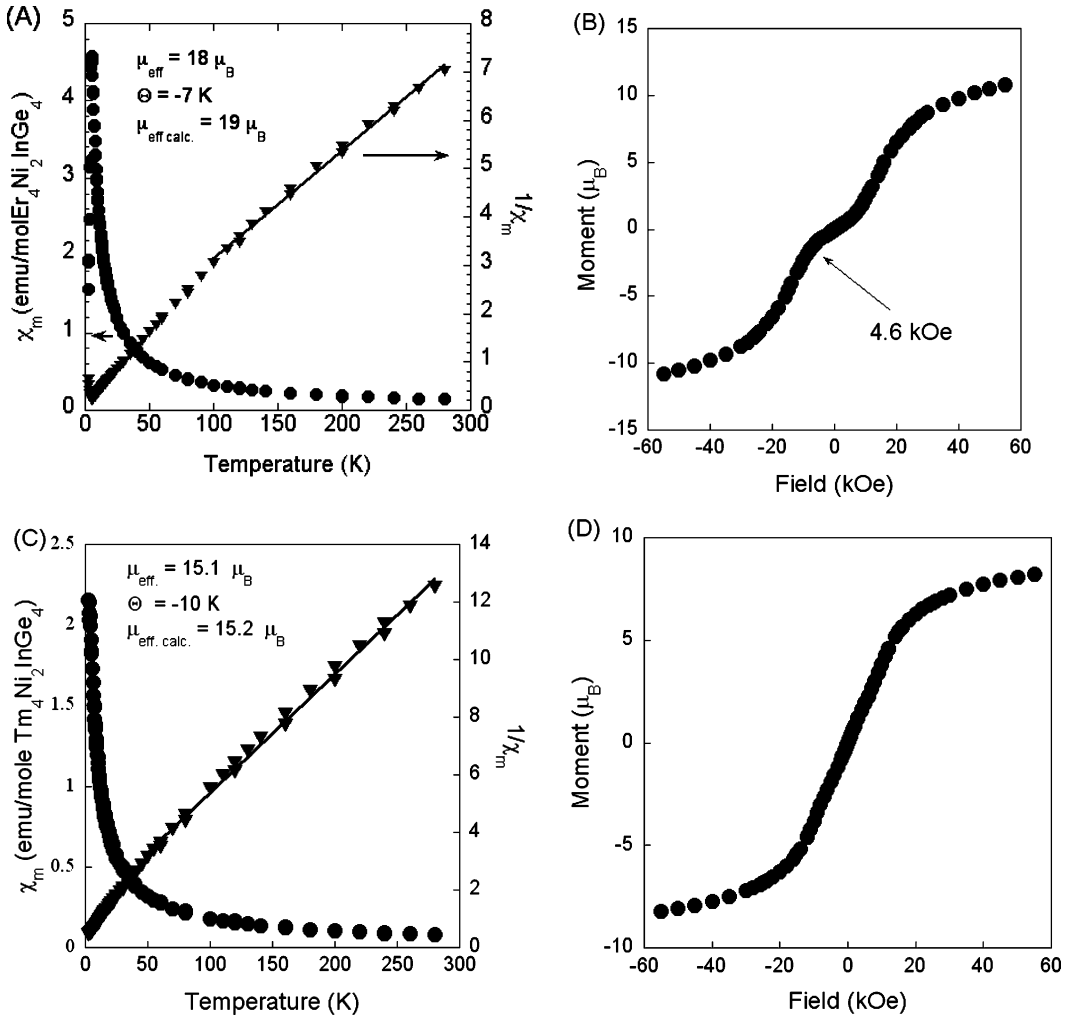

Figure 5. (A) Magnetic and inverse susceptibility data for $Er_4Ni_2InGe_4$. (B) Field-dependent magnetization data for $Er_4Ni_2InGe_4$ collected at 2 K. (C) Magnetic and inverse susceptibility data for $Tm_4Ni_2InGe_4$. (D) Field-dependent magnetization data for $Tm_4Ni_2InGe_4$ collected at 2 K.

is a change in the behavior, and above this field, the moment has a much stronger dependence, suggesting metamagnetic behavior. Unlike the previous two examples whose moments increased linearly up to 55 kOe, the Er analogue begins to saturate at 30 kOe. At the highest attainable field, the moment only reached about 55% of the saturation value.

(d) $Tm_4Ni_2InGe_4$. The magnetic behavior of the Tm analogue is quite different from that of the previous three analogues. First, there is no maximum in the susceptibility data, but instead the susceptibility continues to increase down to the lowest temperature attainable (2 K; Figure 5C). The inverse susceptibility is a linear function of the temperature from 300 K down to about 50 K, where it begins to negatively diverge. The resulting effective magnetic moment for the region fit to the Curie−Weiss law (between 50 and 300 K) was 15.1 μ_B with a Weiss constant of −10 K. The calculated value for the effective magnetic moment for four Tm^{3+} ions is 15.0 μ_B,[23] which is in excellent agreement with the value that we obtained from the measurements. The negative Weiss constant indicates anitferromagnetically interacting moments, though as mentioned above no maximum was observed in the susceptibility data. The negative divergence in the inverse susceptibility data may be caused by several factors, the most likely of which is crystal-field splitting of the ground-state multiplets of the Tm^{3+} ion.[24]

The magnetization curve for $Tm_4Ni_2InGe_4$ is shown in Figure 5D. Unlike the other three examples, we do not observe any change in the slope of the magnetization curve in the lower field region, consistent with the fact that there was no apparent magnetic order to disrupt. The only change in the slope that occurs is in the higher field region between 15 and 25 kOe, and this is caused by the onset of magnetic saturation. Above 30 kOe, the moment again has a linear dependence on the field although the slope is much shallower. The moment at the highest attainable field is about 8 μ_B, which is about 60% of the value expected for four Tm^{3+} ions.

In all of the compounds measured, the only species that makes a contribution to the paramagnetic susceptibility is the rare-earth atom. The Ni atom apparently has a diamagnetic d^{10} configuration, a common feature of intermetallic compounds containing electropositive elements such as lanthanides and alkaline earths.[1,2,25] These compounds could

(24) Van Vleck, J. H. *The Theory of Electronic and Magnetic Susceptibility*; Oxford University Press: London, 1932.
(25) Vajenine, G. V.; Hoffman, R. *J. Am. Chem. Soc.* **1998**, *120*, 4200−4208.

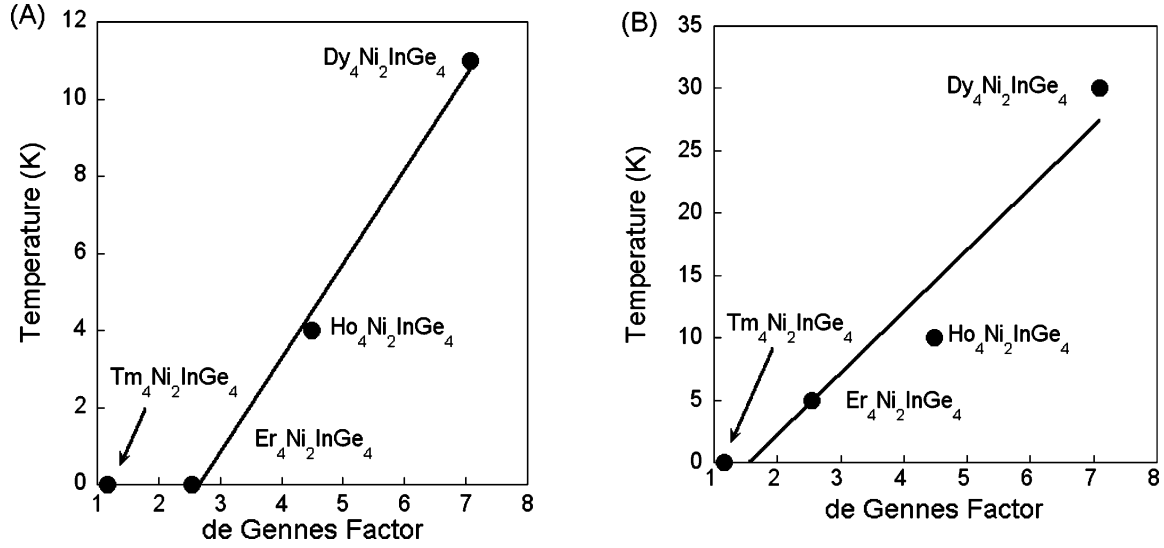

Figure 6. (A) Plot of the de Gennes factor as a function of the lower temperature susceptibility maxima for $RE_4Ni_2InGe_4$. (B) Plot of the de Gennes factor as a function of the higher temperature susceptibility maxima for $RE_4Ni_2InGe_4$.

be best described as polar intermetallics with the following formal charge-balancing scheme $(RE^{3+})_4(Ni_2InGe_4)^{12-}$. The Ni_2InGe_4 substructure is presumably metallic with delocalized electrons.

(e) Origin of the Trend and Dominant Exchange Mechanism. In metallic systems with RE atoms, the dominant mechanisms for magnetic exchange are indirect ones such as Ruderman−Kittel−Kasuya−Yosida (RKKY) coupling.[26] In this scheme, conduction electrons are polarized by the magnetic moments of the RE. This polarization is imparted to adjacent electrons and ultimately to other RE atoms acting to couple the moments either ferromagnetically or antiferromagnetically over long distances. This is the magnetic exchange mechanism found in the RE elements themselves despite the fact that they are in direct contact with one another in the elemental form. This is due to the compact nature of the f orbitals, which precludes direct orbital overlap for exchange.[27] Indeed, we noted above that the RE atoms in the title compounds are quite close to one another, and we infer that RKKY is the magnetic exchange mechanism at work in the title compounds as well.

When RKKY is the dominant exchange mechanism, it is found that the magnetic ordering temperatures (be it ferro- or antiferromagnetic) scale with the magnitude of the moment of the paramagnetic species by the de Gennes factor, a value that is defined in eq 1,[28] where J is the total angular momentum and λ is Lande's factor, which takes into account noncollinear effects of the angular momentum and is defined in eq 2. This model assumes that all other factors remain

$$\mathrm{DG} = (\lambda - 1)^2 J(J+1) \tag{1}$$

$$\lambda = 1 + \frac{J(J+1) - L(L+1) + S(S+1)}{2J(J+1)} \tag{2}$$

constant such as the densities of states of the conduction electrons and fermi surface geometry. This is almost always the case when looking at isostructural RE analogues of intermetallic phases because the rare-earth f electrons do not play a significant role in the states near the fermi level. Parts A and B of Figure 6 show the temperatures where the susceptibility maxima were observed as a function of the de Gennes factor for the lower and higher temperature transitions, respectively. We indeed see that the temperatures vary almost linearly with the de Gennes factor, suggesting that indirect magnetic exchange is dominant in this system.

In the case of the Dy and Ho analogues, which show double maxima in the susceptibility data, this observation can be understood by considering the initial onset of antiferromagnetic order at the upper temperatures, resulting in a maximum in the susceptibility, and may be a result of the moments ordering in different crystallographic directions. The initial ordering is followed by a spin reorientation at a lower temperature, whereby a larger component of the moments order along a particular crystallographic axis and result in a second maximum in the susceptibility. The temperature at which these transitions take place is related to the moment of the rare-earth ion as discussed above.

The other trend that emerges is found in the magnetization data of $Dy_4Ni_2InGe_4$, $Ho_4Ni_2InGe_4$, and $Er_4Ni_2InGe_4$, where the curves show abrupt increases at particular applied fields. This likely corresponds to the breaking of the antiferromagnetic order by the applied field, causing a metamagnetic transition. We see that the field at which the transition takes place decreases from $Dy_4Ni_2InGe_4$ to $Er_4Ni_2InGe_4$, corresponding to a decrease in the temperature of the antiferromagnetic ordering with the late-rare-earth metals. Additionally, the Tm analogue did not order magnetically, and therefore the lack of a transition in the magnetization data is reasonable.

(26) (a) Kasuya, T. *Prog. Theor. Phys.* **1956**, *16*, 45−54. (b) Mitchell, A. H. *Phys. Rev.* **1957**, *105*, 1439−1444. (c) Yosida, K. *Phys. Rev.* **1957**, *106*, 893−898.

(27) Elliot, R. J., Ed. *Magnetic Properties of Rare Earth Metals*; Plenum Press: New York, 1972.

(28) de Gennes, P. G. *C. R. Hebd. Seances Acad. Sci.* **1958**, *247*, 1836−1843.

Concluding Remarks

The compounds $RE_4Ni_2InGe_4$ are the first reported examples representing an ordered quaternary variant of the Mg_5Si_6 structure type. Synthetic investigations tentatively suggest that these compounds may best be produced from a molten In reaction and that the reaction conditions need to be carefully controlled to produce $RE_4Ni_2InGe_4$ in large yields. Specifically, the melt needs to be rich in RE metal in order to form and may point to the kinetic stabilization of the phase by concentration gradients within the melt. Despite the stoichiometric similarities of $RE_4Ni_2InGe_4$ to $RENi_2Ge_2$, α-$RENiGe_2$, $RENiGe_3$, and RE_2InGe_2, all of these phases can be bypassed to produce $RE_4Ni_2InGe_4$ exclusively. This example, in conjunction with the β-$RENiGe_2$ case, illustrates the promising nature of In flux to produce novel intermetallics.

That the $RE_4Ni_2InGe_4$ family forms in molten In demonstrates a parallel between phases formed in these molten metal conditions and those that form in metallurgical processing resulting in metal matrix composites.[29] Studying molten metal reactions could potentially be useful in elucidating phases that form at electrical junctions at much lower temperatures between In, Ge, and other metals and how they might relate to the junction performance.

The Ho and Dy analogues exhibit antiferromagnetic ordering at low temperatures. The Dy and Ho analogues seem to undergo a second transition at lower temperature, which is likely due to a spin reorientation. This ordering can be readily disrupted by the application of a magnetic field, resulting in a metamagnetic transition. Future work with this system should include neutron diffraction above and below the different ordering temperatures to better understand the nature of the magnetic ordering, ac susceptibility, and transport measurements such as electrical conductivity.

Acknowledgment. Financial support from the Department of Energy (Grant DE-FG02-99ER45793) is gratefully acknowledged. Part of this work was carried out at the Center for Advanced Microscopy and the Center for Sensor Materials at Michigan State University.

Supporting Information Available: Tables of crystallographic details, atomic coordinates, isotropic and anisotropic thermal displacement parameters for all atoms, and interatomic distances and angles for $Dy_4Ni_2InGe_4$, $Ho_4Ni_2InGe_4$, $Er_4Ni_2InGe_4$, and $Tm_4Ni_2InGe_4$ (CIF). This material is available free of charge via the Internet at http://pubs.acs.org.

IC0605017

(29) Suresh, S.; Mortensen, A. *Fundamentals of Metal Matrix Composites*; Butterworth-Heinemann: Boston, 1993.